J|A|C|S
ARTICLES
Published on Web 09/20/2005

How Enzyme Dynamics Helps Catalyze a Reaction in Atomic Detail: A Transition Path Sampling Study

Jodi E. Basner[†] and Steven D. Schwartz*[,†,‡]

Contribution from the Department of Physiology and Biophysics and Department of Biochemistry, Albert Einstein College of Medicine, 1300 Morris Park Avenue, Bronx, New York 10461

Received November 5, 2004; Revised Manuscript Received May 23, 2005; E-mail: sschwartz@aecom.yu.edu

Abstract: We have applied the Transition Path Sampling algorithm to the reaction catalyzed by the enzyme Lactate Dehydrogenase. This study demonstrates the ease of scaling Transition Path Sampling for applications on many degree of freedom systems, whose energy surface is a complex terrain of valleys and saddle points. As a Monte Carlo importance sampling method, transition path sampling is capable of surmounting barriers in path phase space and focuses simulation on the rare event of enzyme catalyzed atom transfers. Generation of the transition path ensemble, for this reaction, resolves a paradox in the literature in which some studies exposed the catalytic mechanism of hydride and proton transfer by lactate dehydrogenase to be concerted and others stepwise. Transition path sampling has confirmed both mechanisms as possible paths from reactants to products. With the objective to identify a generalized, reduced reaction coordinate, time series of both donor−acceptor distances and residue distances from the active site have been examined. During the transition from pyruvate to lactate, residues located behind the transferring hydride collectively compress toward the active site causing residues located behind the hydride acceptor to relax away. It is demonstrated that an incomplete compression/relaxation transition across the donor−acceptor axis compromises the reaction.

Introduction

The ability of enzymes to specifically accelerate reaction rates a million fold or more when compared to substrate free in solution has inspired research for over a century. Enzyme engineering, for example: de novo protein design, disease dependent modification, inhibition, and regulation of enzyme action all require a detailed understanding of the mechanisms of enzyme catalysis. Molecular dynamics can provide atomistic detail necessary to untangle a catalytic mechanism. The size of macromolecules, however, leads to enormously complicated energy surfaces, consisting of a multitude of "pot-holes", barriers, and transition paths. Molecular dynamics simulation is limited to a few nanoseconds of real time. Additionally, numerical error introduced by rounding and truncation of the integration algorithm, prevent unlimited extension of this time via increased computational speed. Two classes of problems require observation of events on time scales longer than initial value molecular dynamics can provide, namely, rare events and long time dynamics. Even a single dynamic observation of a rare event such as the atom transfers of enzyme catalysis, which occur once every millisecond, has been impossible until recently. Combined with Hybrid Quantum Mechanical/Molecular Mechanical methods[1] (QM/MM), application of the Transition Path Sampling algorithm (TPS)[2] bridges this time-scale gap, generating an ensemble of transition paths, with each path capturing a distinct observation of the rare event. As a Monte Carlo importance sampling method, Transition Path Sampling is equipped to surmount barriers in transition path phase space yielding an equilibrium statistical ensemble of reactive trajectories. This paper presents the first application, to our knowledge, of the Transition Path Sampling algorithm to an enzymatically catalyzed chemical reaction.[3]

The enzyme Lactate Dehydrogenase (LDH) catalyzes the interconversion of the hydroxy-acid lactate and the keto-acid pyruvate with the coenzyme nicotinamide adenine dinucleotide. The reaction catalyzed involves the transfer of a proton between an active site histidine and the C2 substrate oxygen as well as a hydride transfer between NC4 of the coenzyme and C2 of the substrate (Figure 1[4]).

Extensive experimental and computational research concerning the influence of amino acid residues close to the active site on coenzyme binding,[5] substrate binding and orientation, as well as on the reaction event, including ground state destabilization,[6] transition state stabilization,[7] and dynamic coupling[8] has been performed. A main goal of current research on macromolecules

[†] Department of Physiology and Biophysics.
[‡] Department of Biochemistry.

(1) Field, M. J.; Bash, P. A.; Karplus, M. *J. Comput. Chem.* **1990**, *11* (6), 700−733.
(2) Dellago, C.; Bolhuis, P. G.; Geissler, P. L. *Adv. Chem. Phys.* **2002**, *123*, 1−78.
(3) Radhakrishnan, R.; Schlick, T. *PNAS* **2004**, *101* (16), 5970−5975.
(4) Gulotta, M.; Deng, H.; Deng, H.; Dyer, R. B.; Callender, R. H. *Biochemistry* **2002**, *41*, 3353−3363.
(5) Deng, H.; Zhadin, N.; Callender, R. *Biochemistry* **2001**, *40* (13), 3767−3773.
(6) Deng, H.; Zheng, J.; Clarke, A.; Holbrook, J. J.; Callender, R.; Burgner, J. W., II *Biochemistry* **1994**, *33* (8), 2297−2305.
(7) Young, L.; Post, C. B. *Biochemistry* **1996**, *35* (48), 15129−15133.
(8) Basner, J. E.; Schwartz, S. D. *J. Phys. Chem. B* **2004**, *108* (1), 444−451.

10.1021/ja043320h CCC: $30.25

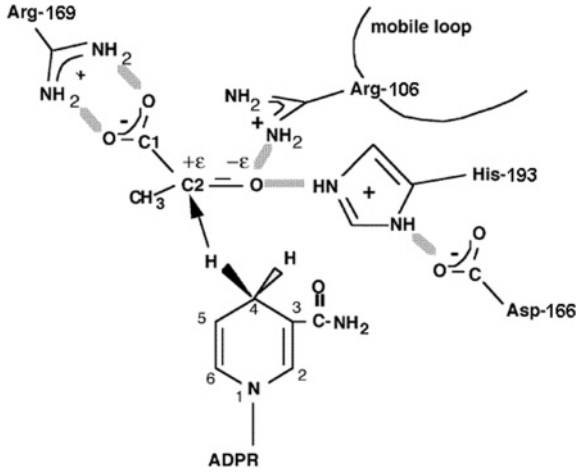

Figure 1. Diagram of the binding site of LDH with bound NADH and pyruvate showing hydrogen bonds between the substrate and key catalytically important residues of the protein. The catalytic event involves the hydride transfer of the NC4 hydrogen of NADH from the pro-R side of the reduced nicotinamide ring to the C2 carbon of pyruvate and protein transfer from the imidozole group of His-193 to pyruvate's keto oxygen. Adapted from ref 4.

is to reduce the enormous number of degrees of freedom, which are on the order of 14 000 for a single LDH subunit, to a smaller affective reaction coordinate. In this effort the collective motions of residues has been clearly demonstrated using methods such as cross correlation maps,[9] principal component analysis,[10] as well as some algorithms developed in our group identifying dynamically coupled motions.[11] The current study focuses on time resolved motions proximate to the reaction event, expanding the definition of the reaction coordinate to include other dimensions that modify the barrier to reaction on a time scale not separable from the reaction coordinate.

TPS offers significant advantageous over other methodologies used to elucidate the mechanism of enzymatic reactions. Previous studies have mapped the potential energy surface of LDH,[12,13] predefining a two dimensional reaction coordinate as the distance of each reactive atom, the hydride and proton, from their respective donor. First, starting structures for different studies were likely located in significantly different regions of the potential energy surface. Many areas on the surface may have the same range of values for the two bonds defining their reaction coordinate, but with distinctly different values of the rest of the degrees of freedom. When those degrees of freedom are minimized, they are *locally* minimized. Therefore, each potential energy surface mapped in previous studies is one small section of the vastly larger total potential energy surface. Second, the studies do not include kinetic energy. It is now accepted, that although it may intuitively seem the reaction would follow the minimum energy path, it is not guaranteed. With kinetic energy the system has the ability to traverse barriers; paths including these barriers would previously be excluded. Third, the reaction coordinate is not sufficiently defined. This and previous work, as mentioned above, have revealed residue motions coupled to the reaction coordinate which must be included in the complete definition of the reaction coordinate. This would mean that if a potential energy surface were mapped, additional parameters would have to be restrained while allowing those degrees of freedom which do not influence the reaction events to minimize. TPS offers an alternative, more tractable, approach. First, since TPS is capable of surmounting barriers in path space, the system is not confined to one sub-area of the energy surface. Second, kinetic energy is included thereby avoiding the exclusion of relevant transition paths. Third, no assumptions restricting the definition of the reaction coordinate are necessary.

Previous work in our group on the LDH isoforms identified and compared periodic motions local to the active site which are coupled to a defined reaction coordinate.[8] Dubbed protein promoting vibrations (PPVs), their incorporation into studies of hydride transfer helped clarify anomalous kinetic isotope effects measured by Klinman and coworkers for a thermophilic Alcohol Dehydrogenase (ADH).[14,15] Quantum tunneling, originally thought to be relevant only at low temperatures, significantly contributes to enzyme catalysis at physiological temperatures via PPVs that drive the transferring atom's donor and acceptor closer together; thereby exploiting tunneling's sensitive dependence on transfer distance. Decreasing of the barrier height due to PPVs, a classical affect, has also been observed in a model system of condensed phase hydride transfer, but with the conclusion that tunneling effects are more significant.[16] Further studies in our group on the human enzyme Purine Nucleoside Phosphorylase (hPNP),[17] which does not accelerate *small* atom transfers, have quantified up to a 20% decrease in barrier height due to a periodic oxygen stack compression. Therefore, although the transferring atoms cannot tunnel in this study,[18,19] the PPV still contributes to the modification of the classical barrier.

The structure of this paper is as follows: Detailed explanations of the implementation of TPS are provided in the Methods section. In the Results section the ensemble of transition paths are examined to further reveal the role of dynamics in enzyme catalysis. The timing of the hydride and proton transfers will be shown to be more variable than previously considered, where subtle changes in residue motions reflect this variability. Enzyme wide changes during the transition, visualized as a compression and relaxation of residues along the hydride donor−acceptor axis, appears to be crucial for reaction completion. As the enzyme heads toward the reactive event, the cofactor and substrate are nudged into alignment with the donor−acceptor axis residues. The compression/relaxation transition is a manifestation of how the overall protein structure creates the PPV. The results demonstrate the application, utility, and advancement TPS provides to molecular simulation.

(9) Luo, J.; Bruice, T. C. *PNAS* **2002**, *99*, 16597−16600.
(10) Amadei, A.; Linssen, A. B. M.; Berendsen, H. J. C. *Proteins: Struct. Funct. Genet.* **1993**, *17* (4), 412−415. Núñez, S.; Wing, D.; Antoniou, D.; Schramm, V. L.; Schwartz, S. D. *J. Phys. Chem. B*, in press.
(11) Mincer, J. S.; Schwartz, S. D. *J. Phys. Chem. B* **2003**, *107* (1), 366−371.
(12) Turner, A. J.; Moliner, V.; Williams, I. H. *PCCP.* **1999**, *1* (6), 1323−1331.
(13) Ranganathan, S.; Gready, J. E. *J. Phys. Chem. B* **1997**, *101*, 5614−5618.
(14) Caratzoulas, S.; Mincer, J. S.; Schwartz, S. D. *J. Am. Chem. Soc.* **2002**, *124* (13), 3270−3276. Kohen, A.; Cannio, R.; Bartolucci, S.; Klinman, J. *Nature* **1999**, *399*, 496−499.
(15) Schwartz, S. D. *Vibrationally Enhanced Tunneling and KIE's in Enzymatic Reactions in Isotope Effects in Chemistry and Biology*; Limbach, H., Kohen, A., Eds.; Marcel Dekker: New York, 2004.
(16) Antoniou, D.; Abolfath, M. R.; Schwartz, S. D. *J. Chem. Phys.* **2004**, *121* (13), 6442−6447.
(17) Núñez, S.; Antoniou, D.; Schramm, V. L.; Schwartz, S. D. *J. Am. Chem. Soc.* **2004**, *126* (48), 15720−15729.
(18) Garcia-Viloca, M.; Truhlar, D. G.; Gao, J. *Biochemistry* **2003**, *42* (46), 13558−13575.
(19) Hammes-Schiffer, S. *Biochemistry* **2002**, *41* (45), 13335−13343.

Methods

Quantum Mechanical/Molecular Mechanical Simulation (QM/MM). We employ the crystal structure of the homotetramic human heart isozyme, h−H_4LDH, in a ternary complex with NADH and oxamate solved by Read et al.[20] at a 2.1 Å resolution (Brookhaven PDB ID: 1I0Z). To generate reactive potential energy surfaces, Quantum Mechanical/Molecular Mechanical calculations were performed on a Linux Cluster using the CHARMM[21]/MOPAC[1] interface with the CHARMM27, all hydrogen force field, and the AM1 semiempirical method. The CHARMM27 force field includes specific parameters for NAD^+/NADH.[22] Oxamate (NH_2COCOO), an inhibitor of LDH, is an isosteric, isoelectronic mimic of pyruvate with similar binding kinetics. Changes to the PDB file included substitution of the oxamate nitrogen with carbon to create pyruvate and replacement of the active site neutral histidine with a protonated histidine to establish appropriate starting conditions with pyruvate and NADH in the active site. A total of 39 atoms were treated with the AM1 potential; 17 or 16 atoms of the NADH or NAD^+ nicotinamide ring, 13 or 12 atoms of the protonated or neutral histidine imidazole ring, and 9 or 11 atoms of the substrate pyruvate or lactate, respectively. PM3 was not used due to errors in parameterization which miscalculate the charge of nitrogen in N−H groups, leading to an incorrect determination of histidine electrostatic potentials.[23] The Generalized Hybrid Orbital (GHO)[24] method was used to treat the two covalent bonds which divide the Quantum Mechanical and Molecular Mechanical regions. The two GHO boundary atoms are the histidine Cα atom and the NC1′ carbon atom of the NAD^+/NADH adenine dinucleotide structure which covalently bonds to the nicotinamide ring. The GHO boundary atom of NAD^+/NADH was chosen based on the CHARMM QM/MM input files from ref 25[25] and the QM/MM calculations on LDH from ref 12. The polarity of the QM/MM bond must be considered when choosing the GHO boundary atom. Although the bond we chose is slightly more polar (NADH:0.43, NAD^+:0.23) than the choice ref 18 made for NADPH (0.24), their choice adds 13 QM atoms, an expense we did not feel necessary for these calculations. Protein structure (PSF) and coordinate (CRD) input files were created with CHARMM. Crystallographic waters were treated as TIP3P[26] residues. A single subunit of the enzyme was used in all QM/MM calculations.

Minimization, equilibration, and dynamics followed a standard protocol. First the structure was minimized using only the CHARMM27 Molecular Mechanical potential for 1000 steps using steepest descent to remove bad van der Waals contacts created by the addition of hydrogens. Then 10 000 further steps of minimization were performed using an adopted-basis Newton−Raphson algorithm (ABNR), achieving a change in energy < 0.001 kcal/mol and a RMS gradient < 0.001 kcal/mol·Å. Then 8 sodium atoms were added to neutralize the −8 overall charge of a single subunit. The enzyme was restrained with a strong force harmonic potential while the sodium atoms were permitted to relax for 400 steps of minimization using an ABNR. The final step of minimization using 500 steps steepest descent and 5000 steps ABNR included the full QM/MM potential assignment discussed above, as did all simulations here-after. The MM-MM nonbonding cutoffs were 14 Å and there were no cutoffs for QM-MM nonbonding interactions. The enzyme was heated to 300 K over 10 ps, equilibrated with velocities assigned from a Gaussian distribution every 100 steps at 300 K for another 10 ps and then dynamically equilibrated for a final 10 ps. The equations of motion were solved using Leapfrog Verlet integration with a 1 fs time step, sufficient with SHAKE constraints.

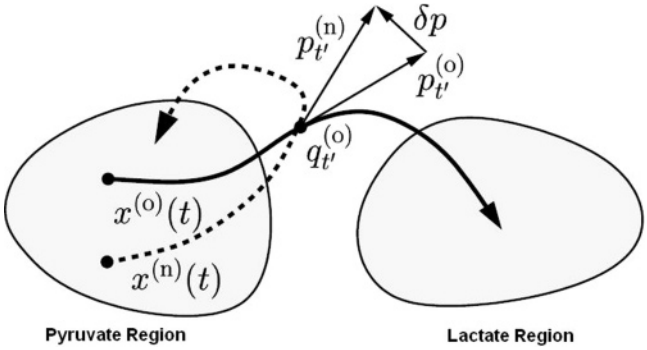

Figure 2. Shooting moves to create new reactive and nonreactive trajectories. The shaded regions represent the nonoverlapping areas in coordinate space defined by the order parameters (see text). $x^{(o)}(t)$ is the old reactive trajectory. $q_{t'}^{(o)}$ and $p_{t'}^{(o)}$ are the coordinates and momenta, respectively, from the randomly selected time slice of the old reactive trajectory used to initiate a shooting move. δp is the momenta displacement that generates the new momenta $p_{t'}^{(n)}$. $x^{(n)}(t)$ is the newly generated nonreactive trajectory, beginning and ending in the Pyruvate Region. A newly generate reactive trajectory would connect the Pyruvate and Lactate Regions. Adapted from ref 2.

Transition Path Sampling (TPS).

Definition of the Order Parameters. The reactive trajectory phase space was divided into three nonoverlapping regions of interest defined by low-dimensional order parameters (Figure 2).

The pyruvate region included all configurations where the bond length of the reactive proton and the reactive nitrogen of the active site histidine (NE2) was 1.3 Å or shorter and the bond length of the reactive hydride and the reactive carbon (NC4) of the NADH coenzyme was 1.3 Å or shorter. The lactate region included all configurations where the bond length of the reactive proton and the reactive substrate oxygen (O) was 1.3 Å or shorter and the bond length of the reactive hydride and reactive substrate carbon (C2) was 1.3 Å or shorter. The transition region included all configurations where neither of the above combined bond lengths were satisfied. All bond lengths were determined as the maximum over a 4 ps trajectory in each substrate region. Order parameters are a guideline to differentiate regions; 1.3 Å was found to be a viable discriminator. A reactive trajectory was defined as a single dynamics simulation which connected the pyruvate region to the lactate region or vice versa. A nonreactive trajectory connected the same basin, i.e., lactate/lactate or pyruvate/pyruvate.

Generating an Initial Reactive Trajectory. The hydride and proton donor−acceptor distances of an equilibrated structure were restrained with a harmonic force constant of 500 kcal/mol/Å^2 until they were approximately 3 Å each. The hydride and proton were then repositioned at the midpoint of their respective donor−acceptor axis. Velocities taken from a 300 K equilibration run were then used with the above coordinates to initiate simulations both forward and backward in time. Recall, for time reversible deterministic dynamics inverting the sign of each xyz momentum and then integrating forward in time is equivalent to simulating a trajectory backward in time. The hydride initial velocity was slightly altered to move along the donor−acceptor axis. This produced a 500 fs trajectory that began in the reactant well and finished in the product well. We note, high temperature simulations were unsuccessful in generating a reactive trajectory.

TPS/CHARMM Interface. The TPS simulation was implemented entirely within the CHARMM domain. The algorithm required to generate a microcanonical transition path ensemble using deterministic dynamics is well established[2] and will only be reviewed briefly here. The 500 fs initial reactive trajectory discussed above, including both coordinates and momenta, was the input to launch the TPS simulation.

(20) Read, J. A.; Winter, V. J.; Eszes, C. M.; Sessions, R. B.; Brady, R. L. *Proteins: Struct., Funct., Genet.* **2001**, *43*, 175−185.
(21) Brooks, B. R.; Bruccoleri, R. E.; Olafson, B. D.; States, D. J.; Swaminathan, S.; Karplus, M. *J. Comput. Chem.* **1983**, *4*, 187−217.
(22) Gao, J.; Pavelites, J. J.; Bash, P. A.; Mackerell, A. D., Jr. *J. Comput. Chem.* **1997**, *18* (2), 221−239.
(23) Mulholland, A.; Richards, W. G. *Proteins: Struct., Funct., Genet.* **1997**, *27*, 9−25.
(24) Gao, J.; Amara, P.; Alhambra, C.; Field, M. J. *J. Phys. Chem.* **1998**, *102*, 4714−4721.
(25) http://www.psc.edu/general/software/packages/charmm/tutorial/mackerell/qmmm.html.
(26) Jorgensen, W. L.; Chandrasekhar, J.; Madura, J. D.; Impey, R. W.; Klein, M. L. *J. Chem. Phys.* **1983**, *79*, 926−935.

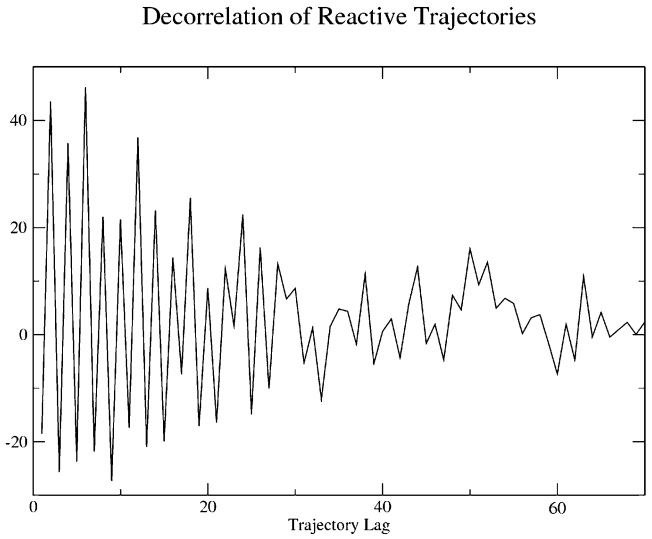

Figure 3. Decorrelation of reactive trajectories. All trajectories were aligned with a reference trajectory so that the hydride transfer occurred at the same time. The XYZ coordinates of the hydride and proton were then taken from within the Transition Region and concatenated into a series. The order of the series followed the order in which the trajectories were generated. This figure is the autocorrelation of the series and demonstrates the decorrelation of the reactive trajectories in about 30 successful shooting trials. Since 1000 shooting attempts were made with a 26% acceptance ratio, this study successfully sampled approximately 8 significantly separated regions of path space.

To generate new reactive trajectories the shooting algorithm was employed (Figure 2). A randomly chosen time slice from the 500 fs trajectory was selected. A small random displacement, chosen from a zero mean Gaussian distribution, multiplied by a constant factor was added to the momenta. The constant factor is used to regulate the ratio of new reactive trajectories to nonreactive trajectories. If this ratio is very high then the shooting trials are possibly moving very slowly through trajectory space. A constant factor of 0.1 achieved a 26.5% acceptance ratio. This constant factor was considered sufficient since the trajectories became uncorrelated in about 30 successful shooting trials (Figure 3, see Analysis). The new momenta were then rescaled to conserve linear momentum, angular momentum, and energy. Components violating the SHAKE constraints were removed. Since we searched within the microcanonical ensemble and used Newtonian dynamics, any configuration generated by this method of perturbing the momenta and conserving energy, linear momentum, and angular momentum while leaving the coordinates undisturbed was guaranteed to satisfy a symmetric generation probability. Therefore, the probability of accepting a new trajectory solely depended on whether the trajectory connected the reactant and product regions defined by the order parameters discussed above. With this new configuration, that is the same coordinates but perturbed momenta, dynamics were run forward and backward in time to complete a 500 fs total time trajectory. The final conformation of both the forward and backward trajectory was determined to be in the Pyruvate, Lactate, or Transition region by its order parameter values. If the new trajectory was reactive then it was accepted to initiate a new shooting move. If the new trajectory was not reactive then the old trajectory was used to initiate a new shooting move. A total of 1000 shooting attempts were made yielding a total of 265 new reactive trajectories. Since the trajectories became uncorrelated after about 30 trajectories, this yields approximately 8 significantly separated reactive regions of path space.

Definitions of Analysis Tools. Prior to presenting our results in detail, we define the mathematical tools we will use to analyze our computational results.

Autocorrelation Function of Trajectory Phase Space. For each reactive trajectory a time series of the distance of the hydride from the NAD^+/NADH reactive carbon was created. Twenty femtoseconds, incorporating the hydride transfer from a selected trajectory, was used as a reference. The time series of each trajectory was then shifted, 1 fs at a time, to determine the minimum RMSD from the reference. The XYZ coordinates of the hydride and proton were taken from the tenth time slice of the 20 fs block with the minimum RMSD, so the enzyme was within the Transition Region. This created a 6-dimensional series in the order in which the trajectories were generated. The autocorrelation of this series is shown in Figure 3. The trajectories became uncorrelated in about 30 successful iterations of the shooting algorithm.

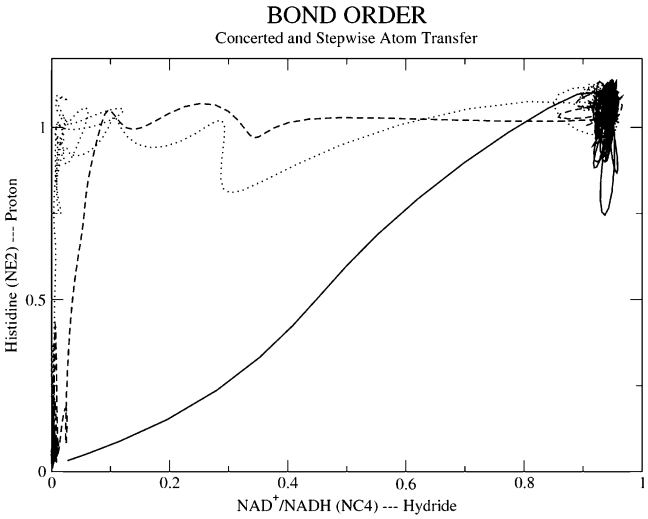

Figure 4. Bond order of the NAD^+/NADH reactive carbon (NC4) with the hydride is plotted versus the bond order of the active site histidine reactive nitrogen (NE2) with the proton for 3 exemplary trajectories generated from the Transition Path Sampling algorithm. Along with Figure 5, it is clear that the LDH mechanism for the hydride and proton transfer can be concerted or stepwise. The solid line shows the bond order for a trajectory where the transfer is concerted (time lag between hydride and proton transfer is less than 10 fs). The dashed line depicts a trajectory with a time lag of 24 fs, and the dotted line depicts a trajectory with a time lag of 195 fs, examples of a stepwise transfer.

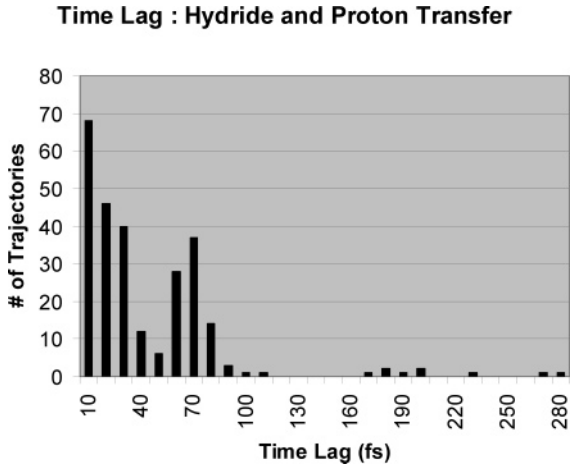

Figure 5. Time lag between hydride and proton transfer. The transition path sampling algorithm moves through trajectory phase space, sampling the myriad of transition barriers. The hydride and proton transfer can be transferred in a concerted or stepwise mechanism. The *x* axis is the difference in time between the hydride and then proton transfer. The *y* axis shows the number of trajectories that were within the particular 10 fs block of time (e.g., 20 indicates that the time lag between the hydride and then proton transfer was between 11 and 20 fs). The majority of transfers occur with a time lag greater than 10 fs, indicating the average mechanism to be stepwise.

Transfer Time. To determine the time lapse between the hydride and proton transfer a time series of the distance of the hydride/proton from both its donor and acceptor was created. The time of transfer for

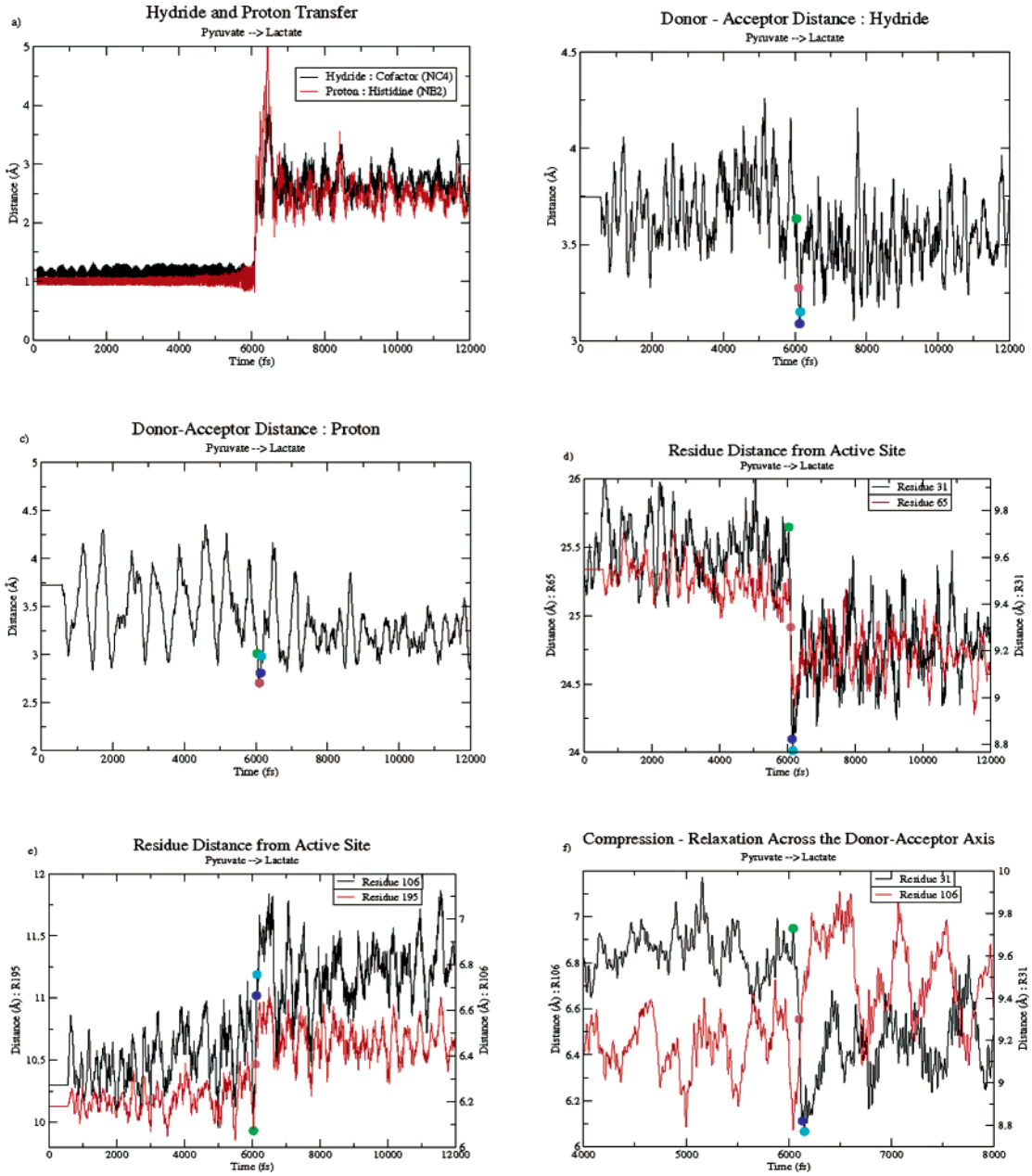

Figure 6. Time series analysis of an exemplary reactive trajectory with a hydride/proton time lag of 7 fs. Various time series of distances are plotted for the pyruvate to lactate reaction direction. The acceptor side residues (106, 195) are closer to the active site with pyruvate bound than when lactate is bound. The opposite is true for the donor side residues (31, 65). To clarify an order of events the minima of each distance are marked on the black time series of panels b−f with colored dots where green = residue 106, brown = proton donor−acceptor distance, blue = hydride donor−acceptor distance, and cyan = residue 31. The acceptor side residues (106, 195) reach their minimum first, then the proton donor−acceptor distance, then the hydride donor−acceptor distance and then the donor side residues (31, 65). The donor side residues pass through their minimum in the pyruvate basin about the time the minimum proton donor−acceptor distance is reached, indicating that the proton donor−acceptor minimum is mainly achieved through the acceptor side residue compression toward the active site. The continued, collective, compression of the donor side residues toward the active site while the acceptor side residues resume an oscillation brings the hydride donor−acceptor residues together, initiates interactions across the donor, transferring atom, and acceptor, and ultimately pushes the acceptor side residues away from the active site. Summarily, an initial compression from both the donor and acceptor side brings the donor−acceptor distances to a minimum, while the continued compression of the donor side residues completes a compression/relaxation event across the hydride donor−acceptor axis.

each atom was taken as the time slice when the hydride or proton was equidistant from their respective donor and acceptor.

Covalent Bond Order. For valence electrons neglect of differential overlap theories such as AM1 the bond order is given by the Wiberg index.

$$\mathrm{BI} = \sum_{a}\sum_{b} P^2_{ab}$$

where P is the density matrix element output by CHARMM, and the summations are over the atomic orbitals of atoms a and b.

Time-Resolved Residue Motions. Select trajectories were extended forward and backward in time to yield a 12 ps trajectory for analysis. Time series of the distance of each residue's center of mass coordinates from the active site were created. Twelve picoseconds is used to highlight that the discussed events only occur proximate to the reactive event. All time series were aligned using the same method described in the autocorrelation function section.

Perturbation of Residue Motions. For this study we have employed a modified version of TPS to determine whether a residue contributes to the reactive event. Rather than perturb the entire configuration, the

residue of interest was selectively perturbed away from the active site (along the residue-active site axis) at a time point close to the reactive event. After the perturbation, the system linear momentum, angular momentum, and energy were scaled to be conserved. The trajectory was analyzed to determine if it remained reactive and what residues were affected by the perturbation.

Results

Bond Order and Transfer Time. Previous studies on LDH mapped the potential energy surface to determine the order of the hydride and proton transfer. One study concluded concerted,[12] another stepwise[13] (where the hydride transfer preceded the proton in the pyruvate to lactate reaction direction), a consequence of the method's limits as discussed in the Introduction. The application of TPS to LDH has revealed both mechanisms of transfer are possible. Figure 4 graphs the bond order of the hydride and the cofactor reactive carbon versus the bond order of the proton and the histidine reactive nitrogen for three trajectories statistically in different parts of phase space.

Figure 5 shows the distribution of the time lag between the hydride and proton transfer for all the reactive trajectories. A total of 74% of the trajectories have a time lag greater than 10 fs (68 $<$ 10 fs, 197 $\geq$ 10). Clearly, the majority of the trajectories proceed via a stepwise mechanism. As we will see in the next sections, subtle changes in the residue motions cause this distribution of time lags.

Enzyme Wide Changes during the Transition from Reactant to Product. Figure 6 graphs various distances that reveal enzyme wide changes that occur proximate to the reaction event for a specific extended trajectory with a time lag between the hydride and proton transfer of about 7 fs.

All graphs are plotted in the pyruvate to lactate reaction direction. All trajectories examined contained this same sequence of events that will be discussed. Our objective for this study is therefore to expose an average quality of the all the harvested trajectories for the purpose of defining a generalized reaction coordinate, as well as, to identify experimental targets for future studies. For parts a−e, 12 ps is plotted to highlight the transition from reactants to products. Part a plots the distance of the hydride from the cofactor reactive carbon and the distance of the proton from the histidine reactive nitrogen. Around 6100 fs, the atoms begin to transfer to the substrate in the conversion of pyruvate to lactate. Parts b and c plot the donor−acceptor distance for the hydride and proton, respectively. The minimum distance of both donor−acceptors, and the distance of residues Valine 31 and Arginine 106 from the active site are marked by color coded points on each graph. The hydride donor−acceptor distance reaches its minimum at 6132 fs (blue), while the proton donor−acceptor distance reaches its minimum at 6100 fs (brown). Part d and e plot the distance of residues 31, 65, 106, and 195, from the active site. Figure 7 shows the alignment of these residues along the hydride donor−acceptor axis, where 31 and 65 are located behind the cofactor and transferring hydride and 106 and 195 are located on the acceptor side behind the substrate.

Viewing the events in a 12 ps window, the residues located behind the transferring hydride compress toward the active site during the transition, while the residues behind the substrate relax away. Part f of Figure 6 plots the distance of residues 31 and 106 from 4 to 8 ps to expose this sequence of events. Residue 106, the Arginine of Figure 1 responsible for polarization of the substrate carbonyl bond via hydrogen bonding, initially compresses toward the active site reaching a minimum distance at 6043 fs (green). By 6153 fs (cyan) residue 31 has reached its minimal compression toward the active site. This combined compression toward the active site is what causes the donor−acceptor of the hydride and proton to reach their minimum, initiating interactions across the donor, transferring atom, and acceptor. The events that occur next are critical for completion of the reaction. The continued compression of the donor side residues toward the active site are not only involved with bringing the donor−acceptor distance closer together, but also with shifting the entire enzyme. While the donor−acceptor distances increase again it will be the motion of the surrounding residues that ultimately determine whether the atoms transfer. The compression of the donor side residues cause the acceptor side residues to relax away and the reaction to complete.

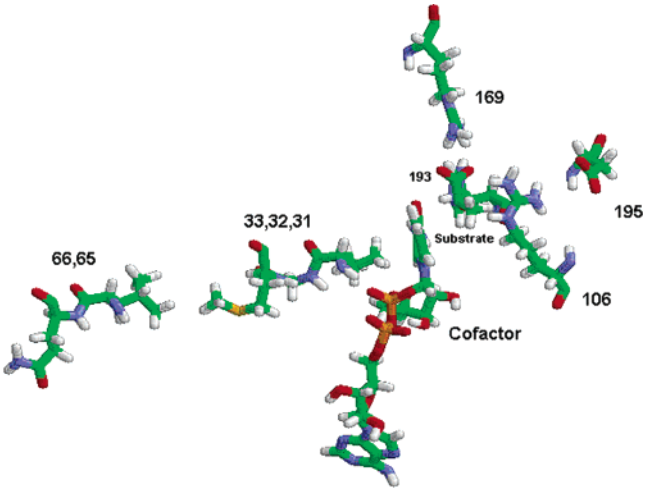

Figure 7. Donor-Acceptor Axis Residues. For the pyruvate to lactate reaction direction residues located behind the cofactor nicotinamide ring (3,66,65,33,32,31) compress toward the active site, while residues located behind the substrate (106,195) relax away. 66 = Gln, 65 = Leu, 33 = Met, 32 = Gly, 31 = Val, 106 = Arg, 195 = Asp, 169 = Arg, 193 = His.

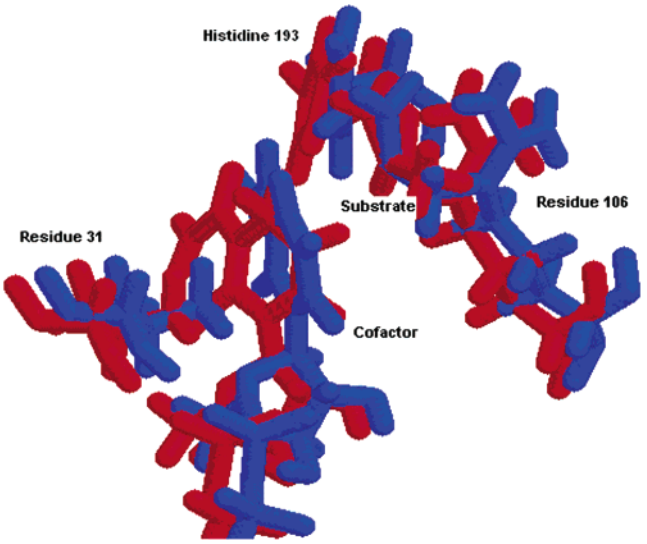

Figure 8. Comparison of snapshots taken during the reactive event (blue) and in the pyruvate basin (red) from the trajectory with a 7 fs time lag between the hydride and proton transfer. Moving toward the reactive event there is reorientation of the donor and acceptor to align with the donor−acceptor axis residues. We can also see in this picture the compression of the residue 31 and the relaxation of residue 106.

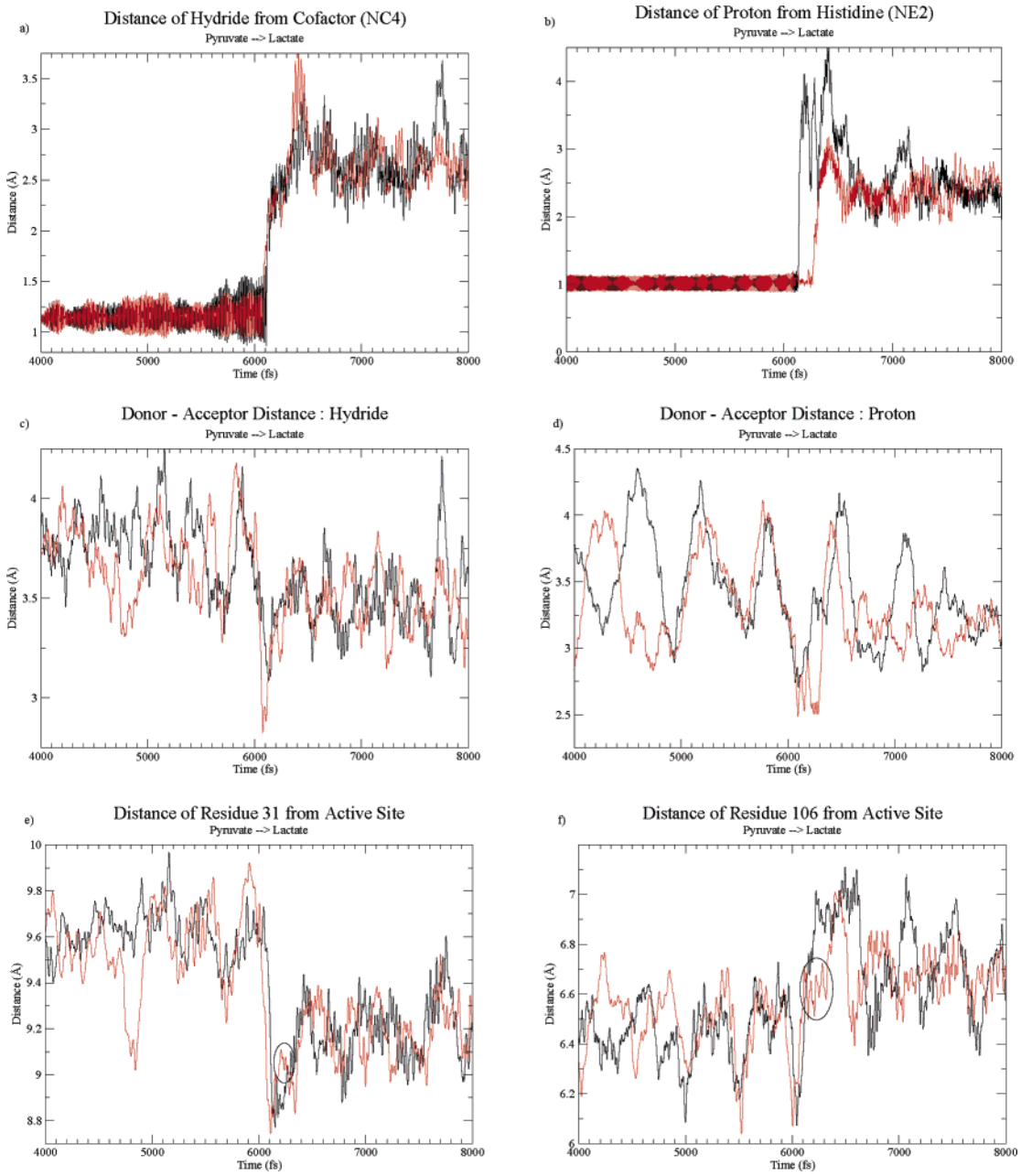

Figure 9. Contrasting concerted and stepwise trajectories. Various time series of distances are plotted for one trajectory with hydride/proton time lag of 7 fs (black) and one trajectory with hydride/proton time lag of 195 fs (red) for the pyruvate to lactate reaction direction. The hydride donor−acceptor distance for the 195 fs time lag trajectory reaches a minimum before the 7 fs trajectory due to the earlier combined compression of residues 31 and 106. The proton transfer of the 195 fs trajectory is delayed due to the sharp retraction of residue 31 from the active site immediately after it has reached its minimum distance from the active site (section of trajectory circled in panel e). This causes a delay in the relaxation of the acceptor side residues (section of trajectory circled in panel f), and therefore a delay in the proton transfer.

Two snapshots of the cofactor, substrate, active site histidine, residue 31 and residue 106 along the reactive trajectory are depicted in Figure 8.

One is from within the pyruvate basin (red) and the other during the atom transfers (blue). The nicotinamide ring of the cofactor twists between these two time points so that the donor and acceptor line up with the donor−acceptor axis residues. It appears once the axis is lined up the reaction can occur.

We note that the donor−acceptor distances are both greater when pyruvate is bound. Previous work related this property to a decreased probability of substrate turnover in the heart isozyme.[8] It is known that the heart isozyme is localized to aerobic tissue where the production of pyruvate is required, while the muscle isozyme is localized to anaerobic tissue such as skeletal muscle.[27,28] It may be that control of product formation occurs via the preferential capability of an isozyme to turnover a particular substrate. Therefore, although the heart and other isoforms of LDH all catalyze reversible reactions, it is possible they are optimally designed to accommodate either pyruvate or lactate. Unfortunately, all the experimental parameters to verify this hypothesis are not yet available.

Contrasting Concerted and Stepwise Trajectories. Figure 9 plots similar distances as the previous section contrasting two

(27) Mathews, C. K.; van Holde, K. E.; Ahern, K. G. *Biochemistry*, 3rd ed.; Addison-Wesley Longman, Inc.: San Francisco, 2000.
(28) Boyer, P. D. *Enzymes* **1975**, Vol. XI, 191−292.

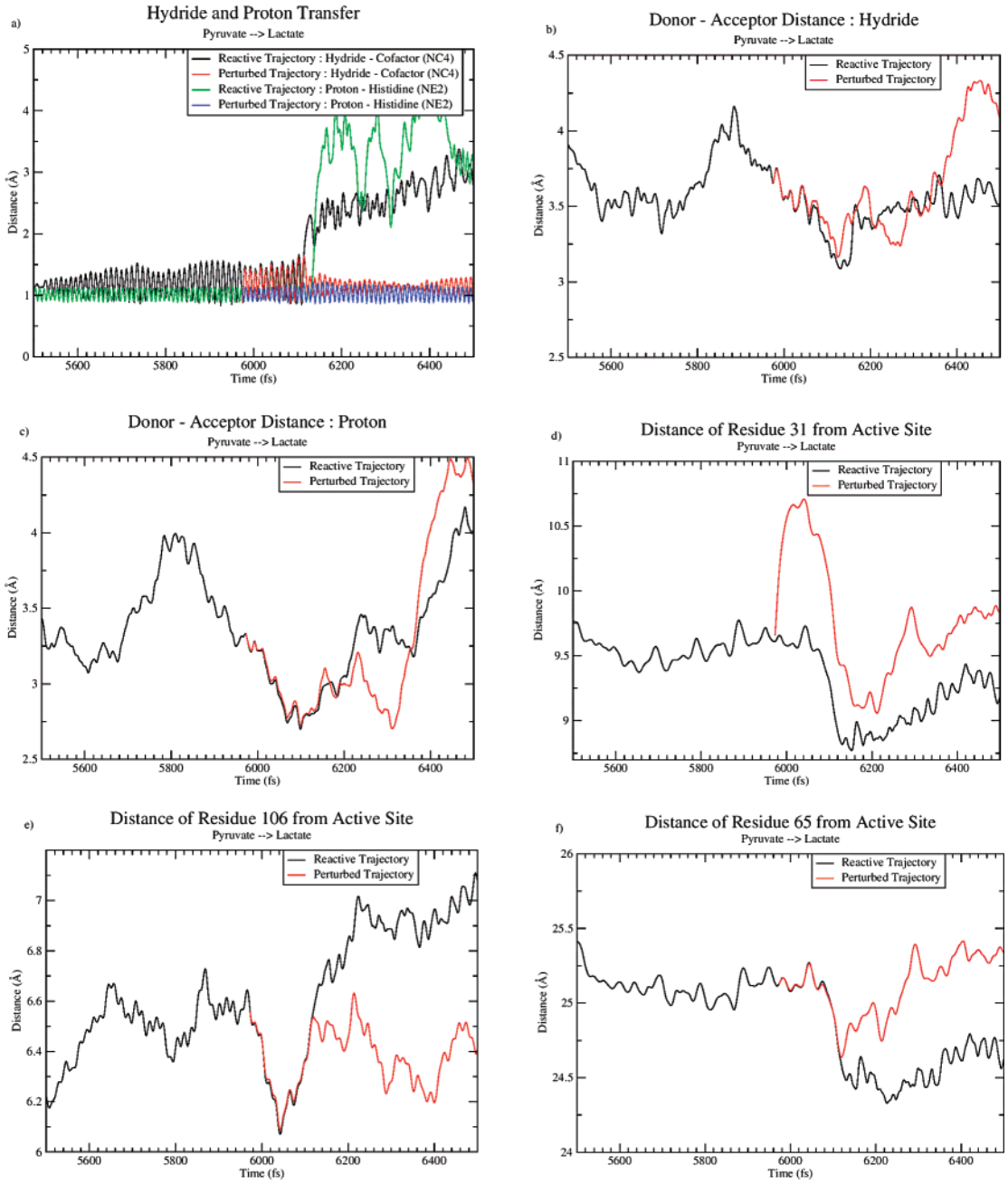

Figure 10. Perturbation of the donor−acceptor axis compression/relaxation reaction coordinate. Various time series of distances are plotted for the trajectory with a hydride/proton time lag of 7s (black/green) and a perturbed trajectory (red/blue) for the pyruvate to lactate reaction direction. Residue 31 is perturbed away from the active site at a time slice 160 fs away from the reactive event. This results in an incomplete initial compression to bring the hydride donor−acceptor atoms to the minimum of the original reactive trajectory. Additionally, the perturbation disrupts the compression/relaxation transition across the donor−acceptor axis, preventing atom transfer.

trajectories: one with a time lag between the hydride and proton transfer of 195 fs (red), a stepwise trajectory, and the previous 7 fs lag trajectory (black).

We can immediately see that the donor−acceptor distance for the stepwise trajectory reaches its minimum earlier due to the earlier combined compression of residues 31 and 106. But why does the proton take longer to transfer? If we look carefully at the distance of residue 31 after it reaches its minimum it then jumps back away from the active site causing a delay in the relaxation of residue 106, and a delay in the increase of the proton donor−acceptor distance. Soon after, residue 106 relaxes away from the active site while the donor−acceptor distance increases, completing the reaction.

Perturbation of the Donor−Acceptor Axis Compression/Relaxation Reaction Coordinate. This section demonstrates the effects of disrupting the compression/relaxation of the donor−acceptor axis residues close to the reactive event. The coordinates and velocities of a time slice 160 fs away from the reactive event of the above trajectory with a 7 fs time lag between the hydride and proton transfer were used for the perturbation. The momenta of residue 31 were perturbed along the residue-active site axis away from the active site. As discussed in the methods, the linear momentum, angular momentum, and energy were then rescaled for conservation. Clearly this is not a statistical analysis, we did not create an ensemble of perturbed trajectories. It provides qualitative support

and clarification of the above results. Figure 10 plots the various distances as before, contrasting the original reactive trajectory with the perturbed. Residue 31 is perturbed about 1 Å away from the active site. After a delay, the hydride donor−acceptor distance begins to deviate from the original reactive trajectory, unable to reach its minimum without the full compression of the donor side residues. Additionally, the absence of the compression thwarts the relaxation of the acceptor side residues. The donor−acceptor distances do still come closer, since at that time residue 106 is still compressing and the perturbed residue 31 has a weaker, delayed compression. As a result of this, the hydride appears to begin to transfer. However, since the compression/relaxation transition does not occur the reaction is not completed.

Discussion

The Transition Path Sampling algorithm has initiated a new era in molecular dynamics. Relatively simple to implement, computational chemistry and biology now have the ability to focus on rare events. The limits of previous methods, confining searches to a sub-area of the potential energy surface, excluding kinetic energy, and making assumptions about the reaction coordinate can be overcome with the application of Transition Path Sampling. The ultimate goal is to determine in atomistic detail the mechanisms of enzyme catalysis in the immediate time vicinity of the reaction; to identify which, when, and how residues of the enzyme are critically involved. This study dissects residue participation in the steps of enzymatic catalysis involving atom transfer, revealing a critical motion visualized as a compression/relaxation across the donor−acceptor axis. Clearly, the concept of the reaction coordinate must be expanded from including only those atoms involved in the atom transfer, i.e., donors, acceptors, and transferring atoms, to also include surrounding residues coupled to the atom transfers. This is akin to the situation found in proton transfer in polar solvents where the reaction coordinate is known to be largely composed of solvent motion rather than the transferring particle itself.[29] In the LDH reaction, the donor−acceptor atoms must first be brought closer together to initiate interactions across the donor, transferring atom, and acceptor. This is achieved through a combined compression toward the active site by the donor and acceptor side residues. While the donor−acceptor distance is increasing, it will be the surrounding residue motions which determine the ultimate outcome of the reaction. The presence of this enzyme wide, collective transition, compared to a substrate free in solution, may be a contributing factor to the enzyme rate acceleration.

Although we were able to distinguish small differences between the concerted and stepwise trajectories which clearly affect the rate of atom transfer, it would be better to identify an experimentally accessible trend, such as frequencies of the residue motions. Preliminary analysis of the power spectra of the distance time series did not, however, reveal any distinct trends. These motions are all around 50−150 cm^{-1} (Figure 11) and although the amplitude and frequency vary small amounts from trajectory to trajectory (not shown) they have not yet revealed any order reflective of the variations in time lag.

However, it is likely the eventual alignment of the donor and acceptor with the donor−acceptor axis that makes the PPV

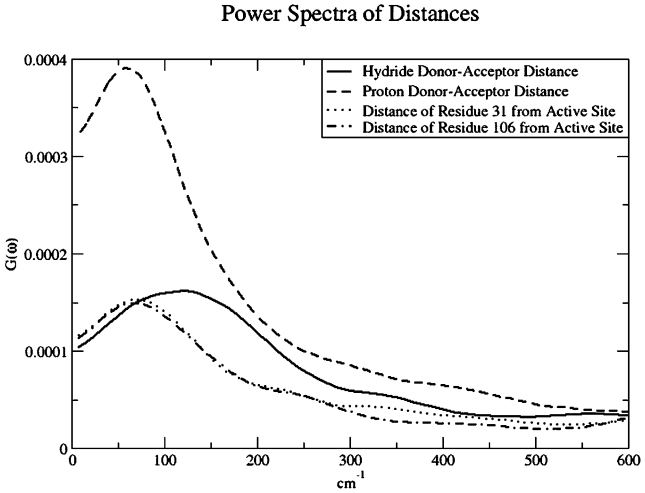

Figure 11. Power spectra of some of the distance plots for the 7 fs time lag trajectory from Figure 6. There is strong coupling between the residue motions and the donor−acceptor distances. With the alignment of the donor and acceptor with the donor−acceptor axis residues the PPV becomes effective. The compression/relaxation transition is a manifestation of how the overall protein structure creates the PPV.

effective. This is a bigger question for an understanding of macromolecules. Is it a statistical opportunity, a fluctuation, which causes the donor and acceptor side residues to compress simultaneously or is the fate of the trajectory set at an earlier time? Analysis outside the scope of molecular dynamics will be necessary to answer this question because time scales longer than that accessible are required.

We note that residue 106 is also part of the LDH loop which closes over the substrate prior to the atom transfers. Experimental studies may be able to detect the compression/relaxation by comparing the rate of loop opening with either pyruvate or lactate bound. It is known that the rate-limiting step for the lactate to pyruvate reaction direction is the loop opening and for the pyruvate to lactate direction it is the loop closing. Since the compression/relaxation for the pyruvate to lactate direction is in the direction of the loop opening, it is possible that this rate will be faster than for the conversion of lactate to pyruvate.

Future studies will determine the separatrices, the phase space dividing surfaces between reactants and products, using commitor distributions. This will verify the donor−acceptor axis residues as part of the reaction coordinate. The complexity of defining reactive and nonreactive regions of phase space (stable and unstable manifolds) will also be investigated.[30]

Transition Path Sampling addresses the fact that many degree of freedom systems have very complicated energy landscapes, and offers a method for us to observe trajectories in atomistic detail to determine atomic motions contributing to a reaction path. There is a need to connect short time motions that can be studied with TPS with long time spatial rearrangements accessible by such methods as position space Monte Carlo. Future studies in our group will address these questions directly by building a broader picture of the energy surface of macromolecules, where the series of significant saddles from the reactant basin to product basin will be mapped and their dynamical correlations considered.

(29) Staib, A.; Borgis, D.; Hynes, J. T. *J. Chem. Phys.* **1995**, *102*, 2487−2505.

(30) Toda, M.; Komatsuzaki, T.; Konishi, T.; Berry, R. S. *Adv. Chem. Phys.* **2005**, 130.

Acknowledgment. We acknowledge the support of the office of Naval Research, The National Science Foundation through Grant No. CHE-0139752, and the NIH through Grant No. GM068036. The authors would like to thank Sara Núñez, Dimitri Antoniou, and Keng Pineda for helpful discussions.
JA043320H